

Implementation of the external complex scaling method in spheroidal coordinates: Impact ionization of molecular hydrogen

Vladislav V. Serov

Department of Theoretical and Nuclear Physics, Saratov State University, 83 Astrakhanskaya, Saratov 410012, Russia

Boghos B. Joulakian

Laboratoire de Physique Moléculaire et des Collisions, Institut Jean Barriol FR CNRS n° 2843, Université Paul Verlaine-Metz, 1 Rue Arago, 57078 Metz Cedex 3, France

(Received 28 May 2009; published 9 December 2009)

We develop an *ab initio* procedure based on the driven Schrödinger equation formalism and the external complex scaling method for the determination of the multifold differential cross sections of the single and double ionization of molecular hydrogen by single photon and fast electron impact. We take advantage of the separability of the two-center Schrödinger equation in prolate spheroidal coordinates in the numerical calculation of the two-electron two-center wave function of the initial and final states of the target. After having verified our procedure by reproducing existing confirmed triple differential cross sections of the $(e, 2e)$ ionization of H_2 , we have extended our calculation to the double ionization of H_2 . Our results on double photoionization agree with existing experimental results. We observe in the mean time a small difference with respect to the absolute results obtained by similar *ab initio* calculations using spherical bases. For the case of the double ionization by fast electron impact for which very few experimental results exist, our results confirm the existing disagreement between the theoretical results and the unique experimental one in the case of $(e, 3-1e)$. This we think makes it clear that for $(e, 3e)$ the introduction of the higher terms of the Born series for mean energy electron-impact regime is necessary.

DOI: [10.1103/PhysRevA.80.062713](https://doi.org/10.1103/PhysRevA.80.062713)

PACS number(s): 34.80.Gs, 33.80.Eh

I. INTRODUCTION

Single- and double-ionization experiments by electron impact which consist in detecting the scattered and the ejected electron(s) in coincidence present singular situations where these complete experiments, in the sense that all the parameters, like energy and momentum vectors are measurable, permit the verification of different theoretical models and approaches. The study of the behavior of the multiply differential cross section of these processes brings answers in many domains like astrophysics, radio damage by secondary electrons in living matter or in plasma physics.

The ionization of H_2 which is the most abundant gas in the universe is particularly interesting for multiple reasons. It can be realized more easily than that of atomic hydrogen, the results can be compared to helium, its double ionization is dissociative and can be used as a source of proton. It also possesses isotopes whose behavior in these experiments gives interesting indication on the vibrational effects.

After the pioneering works on the theory of electron-molecule collisions [1–5] and the early experiments on the $(e, 2e)$ ionization of H_2 [6–9] interest is renewed in recent years on the study of the ionization of diatomic systems, motivated by the evolution of the experimental techniques in the coincidence detection of the fragments produced in an ionization of diatomic molecules by electrons [10,11] or by photons [12–17]. Many theoretical approaches are nowadays available for diatomic targets going from simplest linear combination of atomic transition matrices [18,19] to more elaborate models and procedures like the ones using a two-center Coulomb continuum description based on the Pluvignage [20] type approach [21]. This model was later used to

construct two-electron two-center correlated products in [22] to study the double photoionization $(\gamma, 2e)$ of H_2 and in [23] for the simple $(e, 2e)$. In parallel to these two-center approaches, a one-center model which requires large basis sets are also used in the procedures which try to introduce second-order effects [24,25] and also in a tentative to apply the convergent close-coupling (CCC) approach to the photodouble ionization of H_2 [26]. We must also mention the method using the partial-wave approach constructed by the solutions of the separable Schrödinger equation in prolate spheroidal coordinates [27].

Recently, *ab initio* calculations for the double photoionization of molecular hydrogen were carried out [28–30]. Besides its evident efficiency, this approach presents the advantage of giving an appropriate numerical treatment to the double continuum of the two slow ejected electrons, which is one of the major difficulties of the double-ionization problems. The aim of our paper is to extend the application of this approach to the double ionization by fast electron impact using prolate spheroidal coordinates which by their nature possess the symmetry of the diatomic systems and permit the separation of the two-center one-electron Schrödinger equation.

The outline of the paper is as follows. In Sec. II we present the fundamental aspects of the formalism, in Sec. II B we give the numerical approach. In Sec. III we present and compare our results.

II. THEORY AND PROCEDURE

A. Driven Schrödinger equation

In this section we will develop briefly the procedure based on the formalism of the driven Schrödinger equation ([31]

and references therein) and the external complex scaling (ECS) [32] applied to the double ionization by photons [31] and by electrons. We begin with the general expression of the ionization amplitude

$$f(\mathbf{k}) = \langle \varphi_{\mathbf{k}}^{(-)} | \hat{\mu} | \varphi_0 \rangle \quad (1)$$

where φ_0 represents the initial state of the target, $\hat{\mu}$ the perturbation operator for a given process, \mathbf{k} the set of momenta of the ejected electrons, and $\varphi_{\mathbf{k}}^{(-)}$ the continuum wave function constructed by the sum of an incident wave and an ingoing spherical wave satisfying the stationary Schrödinger equation

$$(\hat{H} - E)\varphi_{\mathbf{k}}^{(-)} = 0. \quad (2)$$

The Hamiltonian of the target can be represented as $\hat{H} = \hat{H}_0 + V$, with $V(\mathbf{r}_1, \dots, \mathbf{r}_{N_e}) = \sum_{i \neq j}^{N_e} \frac{1}{|\mathbf{r}_i - \mathbf{r}_j|}$ the interelectronic potential. Here N_e represents the number of target electrons. $\hat{H}_0 = \sum_{\alpha=1}^{N_e} [-\frac{1}{2}\nabla_{\alpha}^2 + U_{\alpha}(\mathbf{r}_{\alpha})]$, represents the hamiltonian of the electrons in the field of the nuclei represented by the potential $U_{\alpha}(\mathbf{r}_{\alpha})$. The test function $\chi_{\mathbf{k}}^{(-)}$ satisfies the equation

$$(\hat{H}_0 - E)\chi_{\mathbf{k}}^{(-)} = 0. \quad (3)$$

Using the Lippmann-Schwinger equation

$$\chi_{\mathbf{k}}^{(-)} = \varphi_{\mathbf{k}}^{(-)} + \frac{1}{E - \hat{H} - i\epsilon} (-V)\chi_{\mathbf{k}}^{(-)},$$

and replacing for $\varphi_{\mathbf{k}}^{(-)}$, we get

$$\begin{aligned} f(\mathbf{k}) &= \langle [1 + (E - \hat{H} - i\epsilon)^{-1}V]\chi_{\mathbf{k}}^{(-)} | \hat{\mu} | \varphi_0 \rangle \\ &= \langle \chi_{\mathbf{k}}^{(-)} | [1 + V(E - \hat{H} + i\epsilon)^{-1}] \hat{\mu} | \varphi_0 \rangle. \end{aligned}$$

We then use the identity $1 + V(E - \hat{H} + i\epsilon)^{-1} \equiv (E - \hat{H}_0)(E - \hat{H} + i\epsilon)^{-1}$, to arrive to the following expression for the transition amplitude

$$f(\mathbf{k}) = \langle \chi_{\mathbf{k}}^{(-)} | E - \hat{H}_0 | \psi^{(+)} \rangle \quad (4)$$

where the “first-order wave function” $\psi^{(+)}$ satisfies the driven Schrödinger equation

$$(\hat{H} - E)\psi^{(+)} = -\hat{\mu}\varphi_0 \quad (5)$$

with the boundary conditions of an outgoing wave.

We consider then the region $\mathcal{V} \in \mathfrak{R}^{3n_e}$ in the configuration space with n_e representing the number of ejected electrons. The Hamiltonian in the entire space can be split into two Hermitian operators: one internal

$$\hat{H}_{in} = \begin{cases} \hat{H}_0 + \hat{L}_S, & \mathbf{r} \in \mathcal{V}; \\ 0, & \mathbf{r} \notin \mathcal{V}, \end{cases}$$

and one external

$$\hat{H}_{out} = \begin{cases} 0, & \mathbf{r} \in \mathcal{V} \\ \hat{H}_0 - \hat{L}_S, & \mathbf{r} \notin \mathcal{V}. \end{cases}$$

Here $\mathbf{r} = \{\mathbf{r}_{\alpha}\}_{\alpha=1}^{n_e}$ is the set of radius vectors of the electrons. The Bloch's operator \hat{L}_S , satisfies the Green's formula

$$\int_{\mathfrak{R}^{3n_e}} \varphi \hat{L}_S \psi dV = \frac{1}{2} \oint_{\mathcal{S}} \varphi (\mathbf{n}_S \nabla) \psi dS,$$

where \mathcal{S} represents the surface inclosing the volume \mathcal{V} . Using this separation, we rewrite transition amplitude (4) in the form

$$f(\mathbf{k}) = \langle \chi_{\mathbf{k}}^{(-)} | E - \hat{H}_0 - \hat{L}_S | \psi^{(+)} \rangle_{\mathbf{r} \in \mathcal{V}} + \langle \chi_{\mathbf{k}}^{(-)} | E - \hat{H}_0 + \hat{L}_S | \psi^{(+)} \rangle_{\mathbf{r} \notin \mathcal{V}}.$$

Using the Hermitian property and Eq. (3) we obtain for the internal integral

$$\begin{aligned} \langle \chi_{\mathbf{k}}^{(-)} | E - \hat{H}_0 - \hat{L}_S | \psi^{(+)} \rangle_{\mathbf{r} \in \mathcal{V}} &= \langle \psi^{(+)} | E - \hat{H}_0 - \hat{L}_S | \chi_{\mathbf{k}}^{(-)*} \rangle_{\mathbf{r} \in \mathcal{V}} \\ &= -\langle \psi^{(+)} | \hat{L}_S | \chi_{\mathbf{k}}^{(-)*} \rangle, \end{aligned}$$

and

$$\begin{aligned} \langle \chi_{\mathbf{k}}^{(-)} | E - \hat{H} + V + \hat{L}_S | \psi^{(+)} \rangle_{\mathbf{r} \notin \mathcal{V}} &= \langle \chi_{\mathbf{k}}^{(-)} | \hat{L}_S | \psi^{(+)} \rangle \\ &+ \langle \chi_{\mathbf{k}}^{(-)} | V | \psi^{(+)} \rangle_{\mathbf{r} \notin \mathcal{V}}, \end{aligned}$$

for the external. This permits us to write

$$f(\mathbf{k}) = -\langle \psi^{(+)} | \hat{L}_S | \chi_{\mathbf{k}}^{(-)*} \rangle + \langle \chi_{\mathbf{k}}^{(-)} | \hat{L}_S | \psi^{(+)} \rangle + \langle \chi_{\mathbf{k}}^{(-)} | V | \psi^{(+)} \rangle_{\mathbf{r} \notin \mathcal{V}}. \quad (6)$$

Now, assuming that the volume \mathcal{V} is chosen in such a way that $V \rightarrow 0$ for $\mathbf{r} \notin \mathcal{V}$, we can write

$$f(\mathbf{k}) = i \oint_{\mathcal{S}} (\mathbf{n}_S \cdot \mathbf{j}[\psi^{(+)}, \chi_{\mathbf{k}}^{(-)}]) dS. \quad (7)$$

where

$$\mathbf{j}[\psi, \varphi] = \frac{i}{2} [\psi \nabla \varphi^* - \varphi^* \nabla \psi]$$

represents the probability flux.

In the case of usual Coulomb interaction between electrons $V = 1/|\mathbf{r}_1 - \mathbf{r}_2|$, the third term in Eq. (6) is divergent, but expression (7) produces accurate amplitudes with an overall phase factor, which depends on the volume \mathcal{V} [33,34]. This factor has no effects on any physical observable.

Finally we define the perturbation operator for the single-photon continuous-wave photoionization in the “length form” by

$$\hat{\mu} = \sum_{\alpha=1}^{n_e} \mathbf{e} \cdot \mathbf{r}_{\alpha}, \quad (8)$$

where \mathbf{e} is the polarization vector of the incident radiation. For the fast electron-impact ionization the perturbation will be given by

$$\hat{\mu} = -\frac{2}{K^2} \sum_{\alpha=1}^{n_e} \exp(i\mathbf{K} \cdot \mathbf{r}_\alpha), \quad (9)$$

obtained by the application of the first Born approximation to the incident-scattered electron. Here \mathbf{K} represents the momentum transferred to the target by the projectile.

B. Numerical method

Let's consider a diatomic molecule with fixed internuclear vector $\mathbf{R} = R\mathbf{n}_R$. The nuclear attraction potential in the case of H_2^+ and H_2 is given by

$$U(\mathbf{r}) = -\frac{1}{\left| \mathbf{r} - \frac{\mathbf{R}}{2} \right|} - \frac{1}{\left| \mathbf{r} + \frac{\mathbf{R}}{2} \right|}$$

We employ the confocal elliptic (prolate spheroidal) coordinates

$$\xi = \frac{\left| \mathbf{r} - \frac{\mathbf{R}}{2} \right| + \left| \mathbf{r} + \frac{\mathbf{R}}{2} \right|}{R} \in [1, \infty);$$

$$\eta = \frac{\left| \mathbf{r} - \frac{\mathbf{R}}{2} \right| - \left| \mathbf{r} + \frac{\mathbf{R}}{2} \right|}{R} \in [-1, 1]; \quad \phi \in [0, 2\pi).$$

The stationary Schrödinger equation for single-electron two Coulomb center systems like H_2^+ is separable in this system of coordinates, which contain by their nature the diatomic symmetry of the problem. We have thus made the choice to use it in contrast to the choice made in [28–30], which apply for the same molecule the spherical coordinates. The advantage of our choice appears also in the fact that the singular points of the two-center potential are situated on $\xi=1$. Our method differs mainly by this choice and we will thus refer to it as prolate spheroidal external complex scaling (PSECS). Recently, ECS for driven Schrödinger equation in prolate spheroidal coordinate was already implemented [35] but only for photoionization of molecular ion H_2^+ .

We solve Eq. (5) for a given electronic state designated by the eigenvalue M of the z component of the total angular momentum of the two electrons using the expansion

$$\psi_M^{(+)}(\mathbf{r}_1, \mathbf{r}_2) = \sum_m \sum_{l_1=|M-m|}^{N_l-1+|M-m|} \sum_{l_2=|m|}^{N_l-1+|m|} \sum_{j_1, j_2=1}^{N_\xi} \psi_{M m j_1 j_2 l_1 l_2} \varphi_{j_1 l_1, M-m}(\xi_1, \eta_1, \phi_1) \varphi_{j_2 l_2, m}(\xi_2, \eta_2, \phi_2), \quad (10)$$

where

$$\varphi_{jlm}(\xi, \eta, \phi) = b_{mj}(\xi) Y_{lm}(\arccos \eta, \phi).$$

The “radial” basis is given by B -splines of order k , modified for accordance with square-root asymptotics at $\xi \rightarrow 1$ for $m \neq 0$

$$b_{mj}(\xi) = \begin{cases} b_j^k(\xi), & \text{if } m \text{ is even;} \\ \frac{\sqrt{\xi^2 - 1}}{\xi} b_j^k(\xi), & \text{if } m \text{ is odd.} \end{cases}$$

Herein, N_ξ is the number of B -splines per radial dimension, N_l is the number of spherical harmonics per electron. Note that l is the angular-momentum quantum number only at $\xi \rightarrow \infty$. The set with size N_m of m , the eigenvalue of the component of the angular momentum parallel to the molecular axis, is chosen in such a way as to respect the symmetry of the wave function.

We use Neumann's expansion [36] for the electron-electron interaction in prolate spheroidal coordinates

$$\frac{1}{|\mathbf{r}_1 - \mathbf{r}_2|} = \sum_{\mu=-\infty}^{\infty} \sum_{\lambda=|\mu|}^{\infty} U_{\lambda\mu}(\xi_1, \xi_2) Y_{\lambda\mu}(\arccos \eta_1, \phi_1) \times Y_{\lambda, -\mu}(\arccos \eta_2, \phi_2), \quad (11)$$

where

$$U_{\lambda\mu}(\xi_1, \xi_2) = \frac{8\pi}{R} \left[\frac{(\lambda - \mu)!}{(\lambda + \mu)!} \right] P_\lambda^\mu(\xi_<) Q_\lambda^\mu(\xi_>), \quad (12)$$

Here $P_l^m(x)$ and $Q_l^m(x)$ represent respectively the regular and irregular Legendre functions [37]. As in the expansion of angular wave function (10) is limited by N_l and N_m , we take the limits of Neumann's expansion (11) such that $|\mu| \leq \mu_{\max} \leq N_m - 1$, $\lambda \in [\mu_{\max}, \mu_{\max} + \lambda_{\max}]$, $\lambda_{\max} \leq N_l - 1$. As a result, we obtain a linear system with a sparse matrix

$$(\mathbf{H}_1 \otimes \mathbf{S}_2 + \mathbf{S}_1 \otimes \mathbf{H}_2 + \mathbf{U}_{12} - E \mathbf{S}_1 \otimes \mathbf{S}_2) \cdot \boldsymbol{\psi} = \mathbf{f} \quad (13)$$

Here $\mathbf{S}_{\alpha s}$ represent single-particle overlap matrices with elements

$$\begin{aligned} S_{jlm, j'l'm'} &= \langle jlm | j'l'm' \rangle \\ &= \frac{R^3}{8} \int \varphi_{jlm}^* \varphi_{j'l'm'}(\xi^2 - \eta^2) d\xi d\eta d\phi \\ &= \frac{R^3}{8} \delta_{mm'} \left[\delta_{ll'} \int_1^{\xi_{\max}} b_{mj} \xi^2 b_{mj'} d\xi \right. \\ &\quad \left. - \langle lm | \eta^2 | l'm' \rangle \int_1^{\xi_{\max}} b_{mj} b_{mj'} d\xi \right] \end{aligned} \quad (14)$$

and $\mathbf{H}_{\alpha s}$ single-particle Hamiltonian matrices having the elements

$$H_{jlm,j'l'm'} = \frac{R}{4} \delta_{mm'} \delta_{ll'} \times \left\{ \int_1^{\xi_{\max}} b'_{mj}(\xi^2 - 1) b'_{mj'} d\xi + \int_1^{\xi_{\max}} b_{mj} \left[\frac{m^2}{\xi^2 - 1} + l(l+1) - \frac{RZ_+}{2} \xi \right] b_{mj'} d\xi \right\}.$$

We put the total nuclear charge $Z_+=2$ for H_2 .

The solution of the system of linear Eq. (13) is obtained by the conjugate gradient (CG) method with preconditioning matrix

$$\tilde{\mathbf{A}} = \mathbf{H}_1 \otimes \mathbf{S}_2^D + \mathbf{S}_1^D \otimes \mathbf{H}_2 - E\mathbf{S}_1^D \otimes \mathbf{S}_2^D$$

where \mathbf{S}^D represents the diagonal part of \mathbf{S}^D with respect to the index l , $S_{jlm,j'l'm}^D = S_{jlm,j'l'm} \delta_{ll'}$, while \mathbf{S} is three diagonal by l .

Photoionization perturbation operator (8) can be represented via Σ and Π waves [30]. Similarly, first Born operator (9) in the right-hand side of Eq. (5) can be expressed via the plane-wave expansion [38] in prolate spheroidal coordinates.

$$\exp(i\mathbf{K}\mathbf{r}) = 4\pi \sum_{M=-\infty}^{\infty} \sum_{L=|m|}^{\infty} Y_{KLM}^*(\theta_{KR}, \varphi_{KR}) i^L Y_{KLM}(\arccos \eta, \varphi) \times j e_{ML} \left(\frac{KR}{2}, \xi \right), \quad (15)$$

where the $j e_{ml}(c, \xi)$ is the elliptic Bessel function and the ‘‘spheroidal harmonics’’

$$Y_{Klm}(\theta, \varphi) = S_{ml} \left(\frac{KR}{2}, \cos \theta \right) \frac{\exp(im\varphi)}{\sqrt{2\pi}}; \quad (16)$$

$$Y_{0lm}(\theta, \varphi) = Y_{lm}(\theta, \varphi),$$

are defined via prolate angular spheroidal function $S_{ml}(c, \eta)$ [39]. The ‘‘first-order wave function’’ can be constructed by the partial waves

$$\psi^{(+)}(\mathbf{r}_1, \mathbf{r}_2; \mathbf{K}) = \sum_{LM} \psi_{LM}^{(+)}(\mathbf{r}_1, \mathbf{r}_2) Y_{KLM}^*(\theta_{KR}, \varphi_{KR}). \quad (17)$$

The limits of this expansion were chosen according to the modulus K of the momentum transfer. In the calculations concerning the simple ($e, 2e$) ionization we have taken partial waves up to $L_{\max}=4$, $M_{\max}=3$ in the case of $\theta_s=1^\circ$ ($K=0.3233$), and $L_{\max}=5$, $M_{\max}=4$ for $\theta_s=3^\circ$ ($K=0.9087$). In the ($e, 3e$) calculations we have $K=0.6682$ a.u. and we assumed $L_{\max}=4$, $M_{\max}=4$.

To unify and make clearer radial grid definition, we introduce an accessorial variable $\tilde{r} = \frac{R}{2}(\xi - 1)$. In all calculations below, except DPI calculations, we have used cubic B -splines on a uniform mesh, with step $\Delta\tilde{r}=0.5$ and $\tilde{r}_{\max}=50$, which makes the number of splines $N_\xi=103$. Parameters of the angular basis were chosen $N_l=6$, $N_m^\Sigma=7$ for even M and $N_m^\Pi=6$ for odd M . In DPI calculations, we have used $N_\xi=104$ splines of 4-th order, $N_l=6$, $N_m^\Pi=8$ for Π -wave and $N_m^\Sigma=7$ for Σ -wave. To ensure the outgoing wave boundary condition, following external complex scaling approach [31,32], the contour on the point $\tilde{r}_{ECS}=40$ was turned to complex plane on angle $\theta_{ECS}=45^\circ$. Neumann’s expansion

TABLE I. Convergence of the cross section of H_2 double ionization by 75 eV photons with the mesh step $\Delta\tilde{r}$ and the angular basis parameter N_l . The other parameters applied are: $k=4$, $\tilde{r}_{\max}=50$, $\tilde{r}_{ECS}=40$, $\theta_{ECS}=45^\circ$, $N_m^\Pi=2(N_l-2)$, $N_m^\Sigma=N_m^\Pi-1$, $\lambda_{\max}=N_l-1$, $\mu_{\max}=N_m^\Pi/2$, and $\tilde{r}_S=38$.

N_l	$\Delta\tilde{r}$		
	1.0	0.5	0.333333
4	3165.03	3034.37	3028.05
5	2963.59	2836.08	
6	2899.06	2773.35	
7	2891.90		

[36] was restricted to $\lambda_{\max}=N_l-1$, $\mu_{\max}=N_m^\Pi/2$. For such parameters, the CG method converged after about 20–30 iterations to a relative discrepancy of 10^{-6} . In ($e, 2e$) calculations, we used smaller angular basis: $N_m=3$ for $M=0$ and $N_m=2$ for other values of M , $N_l=6$, $\lambda_{\max}=3$ and $\mu_{\max}=1$. We observe that larger numbers about 60–70 iterations in CG were required to attain the same relative discrepancy. This is apparently due to the fact that the final energy $E < 0$ is below double-ionization threshold. The comparison between cross sections calculated with different basis sizes (see Table I) and other scheme parameters (the radius of the space box \tilde{r}_{\max} , the complex scaling angle θ_{ECS} , the turning point \tilde{r}_{ECS} , and the amplitude extraction radius \tilde{r}_S) shows that the numerical error in our calculations is inferior to 2% for DPI calculations and 5% in ($e, 3e$) calculations.

We begin by calculating the wave function for the bound state of H_2 , which will be used as initial-state function φ_0 in the right-hand side of Eq. (5). Being the eigenfunction of the same Hamiltonian matrix it is orthogonal to the final-state function in Eq. (1). We use the continuous analog of Newton’s method (CANM) [40] which produces in each step a system of linear equations of the same type as in Eq. (13). For the internuclear distance $R=1.4$ Bohr and the above mentioned basis parameters for DPI calculations, we have obtained Born-Oppenheimer energy $E_{H_2} = -1.174 19$ Hartrees, while the precise value $E_{H_2} = -1.174 475 714 220$ [41].

C. Amplitude extraction

The test function for single ionization with the formation of H_2^+ in (nlm) state in the united atoms designation is given by

$$\chi_{\mathbf{k}nlm}^{(-)}(\mathbf{r}_1, \mathbf{r}_2) = \chi_{\mathbf{k}}^{(-)}(\mathbf{r}_1) \varphi_{nlm}(\mathbf{r}_2), \quad (18)$$

where $\varphi_{nlm}(\mathbf{r})$ represents the wave function of H_2^+ in the discrete electronic state, and $\chi_{\mathbf{k}}^{(-)}(\mathbf{r})$ the two-center continuum wave function for the momentum \mathbf{k} and the screened charge $Z_+=1$. The natural choice of the surface \mathcal{S} in Eq. (7) is the spheroid defined by $\xi = \xi_S$. The component of the flux on the unit vector of $d\mathcal{S}$ takes the form

$$j_{\xi} dS = \frac{R}{4} (\xi_S^2 - 1) \left[\chi_{\mathbf{k}}^{(-)*} \frac{\partial \psi_{\mathbf{k}nlm}}{\partial \xi_1} - \psi_{\mathbf{k}nlm} \frac{\partial \chi_{\mathbf{k}}^{(-)*}}{\partial \xi_1} \right] \Big|_{\xi_1 = \xi_S} d\eta_1 d\phi_1,$$

where $\psi_{\mathbf{k}nlm}(\mathbf{r}_1) = \langle \varphi_{nlm}(\mathbf{r}_2) | \psi^{(+)}(\mathbf{r}_1, \mathbf{r}_2) \rangle$. The two-center continuum wave function is given as the sum of the spheroidal partial waves

$$\chi_{\mathbf{k}}^{(-)}(\mathbf{r}) = (2\pi)^{3/2} 4\pi \sum_{lm} Y_{klm}^*(\theta_k, \phi_k) i^l e^{-i\delta_{klm}} T_{ml} \left(\frac{kR}{2}, \xi \right) \times Y_{klm}(\arccos \eta, \phi), \quad (19)$$

where $T_{ml}(\xi)$ represent the ‘‘radial’’ Coulomb spheroidal functions [39], and δ_{klm} the phase shifts. Here $T_{ml}(c, \xi)$ and $S_{ml}(c, \eta)$ are obtained by the numerical solution of the separated equations,

$$\left[\frac{d}{d\xi} (\xi^2 - 1) \frac{d}{d\xi} + RZ_+ \xi - \frac{m^2}{\xi^2 - 1} + c^2 \xi^2 + A_{ml}(c) \right] T_{ml}(c, \xi) = 0;$$

$$\left[\frac{d}{d\eta} (1 - \eta^2) \frac{d}{d\eta} - \frac{m^2}{1 - \eta^2} - c^2 \eta^2 - A_{ml}(c) \right] S_{ml}(c, \eta) = 0,$$

using B -splines and Legendre polynomial bases, respectively, with the same grid and basis size as in Eq. (10).

The test function for double ionization is just the product

$$\chi_{\mathbf{k}_1 \mathbf{k}_2}^{(-)}(\mathbf{r}_1, \mathbf{r}_2) = \chi_{\mathbf{k}_1}^{(-)}(\mathbf{r}_1) \chi_{\mathbf{k}_2}^{(-)}(\mathbf{r}_2). \quad (20)$$

Following [31], both functions are defined for $Z_+ = 2$. The surface \mathcal{S} is assumed to be a ‘‘hyperspheroid’’ satisfying $(\xi_1 - 1)^2 + (\xi_2 - 1)^2 = (\xi_S - 1)^2$. The amplitude evaluation radius $\bar{r}_S = \frac{R}{2} (\xi_S - 1) = 38$ Bohr was applied both for single and double-ionization calculations in all examples below.

To explain why we have used fourth-order B -splines for DPI calculation, we must say that a small overlap term appears when the integration is performed over the hypersphere between probe function (20) of double continuum and the single-ionization states. Emphasize, that the numerically evaluated H_2^+ continuum functions used in Eq. (20) are exactly (up to machine accuracy) orthogonal to H_2^+ bound states functions, and overlap arises only due to integration over curved hypersurface. We have seen that this artifact is very sensitive and depends on the smoothness of the derivatives of the wave function and probe function in Eq. (7). So for cubic B -splines, which have a discontinuity on the third order derivative, this overlap term manifests itself as small oscillations in the calculated cross section. The magnitude of these oscillations is in general smaller than the numerical error and usually does not affect the results, but for some cases, such as for the determination of the variation of a asymmetry parameter β with ejection energy, these oscillations are clearly seen. To avoid this we have applied fourth-order B -splines for DPI calculation, which as we observed eliminates the oscillations.

III. RESULTS

To test our procedure we have calculated single photoionization cross section of H_2 , whose values are well established

TABLE II. Total photoionization cross section of H_2 (in Mb)

Photon energy (eV)	ECSPS	Expt. ^a
21.0	6.86	6.77 ± 0.20
26.0	3.92	3.85 ± 0.12
36.45	1.39	1.36 ± 0.04
75.0	0.124	0.124 ± 0.004

^a[42].

both experimentally and theoretically. In Table II we compare the calculated total photoabsorption cross section of H_2 with tabulated experimental values from [42] for several photon energies ω . Here, the same parameters of the numerical scheme were used as in the DPI calculations presented below, except for the case of $\omega = 36.45$ eV (that corresponds to the ejection energy $E_e = 20$ eV), for which we have used the same parameters as in (e,2e) calculations. For $\omega = 75$ eV, only the five lowest single-ionization channels (i.e., with rest H_2^+ ion in $1s\sigma_g$, $2p\sigma_u$, $2p\pi_u$, $2p\bar{\pi}_u$, and $2s\sigma_g$ states) cross sections and the double-ionization cross section were taken into account in the total cross-section calculation. For the other cases, all the open channels are accounted for. It can be seen that the difference between the calculated and experimental values is within the experimental error.

Next, we have calculated the threefold differential cross section (3DCS) for the fast electron-impact single ionization of Helium by assuming in our program very small $R = 0.002$ a.u. On Fig. 1 we can see that our curve is close to the experimental data [44] and actually coincides with the results obtained by other *ab initio* methods [43,44].

Once this verification done, we passed to the determination of 3DCS of the simple ($e, 2e$) ionization of randomly oriented H_2 ,

$$\sigma^{(3)}(E_i, \theta_s, \phi_s, E_e, \theta_e, \phi_e) = \frac{d^3 \sigma}{dE_e d\Omega_s d\Omega_e} = \oint \sigma^{(5)}(\mathbf{R}) d\Omega_R$$

Here

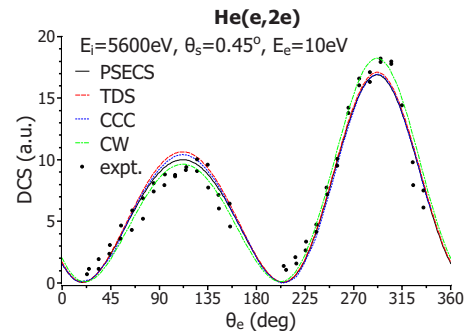


FIG. 1. (Color online) The DCS of the simple ($e, 2e$) ionization of He in terms of the ejection angle θ_e for $E_i = 5600$ eV, $\theta_s = 0.45^\circ$, $E_e = 10$ eV. Present results (solid line), TDS results [43] (dashed line), CCC results [44] (dotted line), CW results (dash-dot line), and experimental data [44] (filled circles).

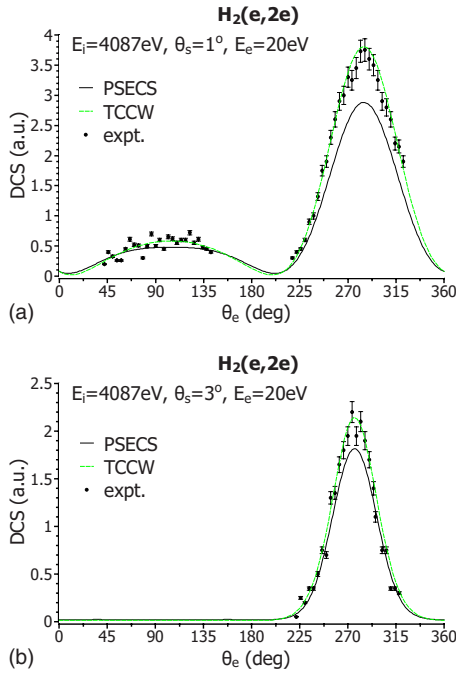


FIG. 2. (Color online) $H_2(e, 2e)$ 3DCS as function of θ_e for $E_i = 4081$ eV, $E_e = 20$ eV: (a) $\theta_s = 1^\circ$ and (b) $\theta_s = 3^\circ$. Present results (solid line), TCCW results [27] (dashed line), and experimental data [9] (filled circles).

$$\sigma^{(5)}(E_i, \theta_s, \phi_s, E_e, \theta_e, \phi_e; \mathbf{R}) = \frac{k_e k_s}{k_i} |f(\mathbf{k}_e, \mathbf{K}; \mathbf{R})|^2$$

represents the 3DCS of the molecule with fixed orientation \mathbf{n}_R of the internuclear axis. In Fig. 2 we compare our results to the experimental [9] and the theoretical [27] two-center Coulomb wave (TCCW) results for two particular values of the scattering angle. We see that the present PSECS underestimates the experimental points, while the TCCW and other approximate methods give results which fit the experiment very well. Comparing to the Helium case, and admitting that the TCCW method is the two-center analog of the Coulomb wave (CW) method for Helium one-center continuum, we can see clearly, that CW results overestimates the 3DCS as TCCW overestimates for H_2 . This suggests that TCCW method is not precise and its agreement with experiment rather casual. On the other hand, our results for the total photoionization cross section for the same ejection energy (see third row of Table II) are in the good agreement with the experimental ones. The difference between the experimental data and our *ab initio* PSECS results for $H_2(e, 2e)$ can be explained by the poor energy resolution (about 4 eV) of the experiment [9]. There is a lot of autoionizing states [45] in the ejection energy region $E_e = 20 \pm 2$ eV. So, this difference can be caused by invalidity of fixed nuclei approximation for such states.

We next pass to the calculation of the cross section of the double photoionization H_2 . We have first of all verified that, results obtained by PSECS agree with the existing theoretical ECS results of [30] which themselves agree with the experimental results of [17] given in absolute value and with [16]

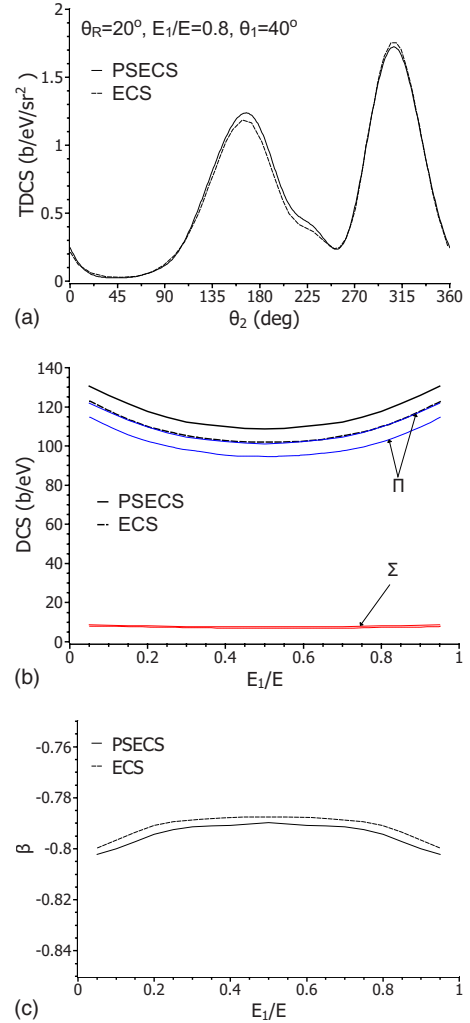


FIG. 3. (Color online) $H_2(\gamma, 2e)$ for photon energy $\omega = 75$ eV: a) TDCS as a function of the ejection angle θ_1 for $E_1 = 0.8E$, $\theta_2 = 40^\circ$, angles between the polarization direction and the molecular axis $\theta_R = 20^\circ$, $\phi_R = 0^\circ$; (b) DCS as a function of the ejection energy E_1 (thick black lines) and its Σ_u and Π_u contributions (thin red and blue lines); (c) The parameter β as a function of the ejection energy E_1 . Our results (solid lines) and ECS results in spherical coordinates [30] (dashed lines).

given in arbitrary units. As we can see on Fig. 3(a) the two curves corresponding to the variation of the TDCS for an aligned H_2 molecule

$$\sigma^{(3)}(\omega, E_1, \theta_1, \phi_1, \theta_2, \phi_2; \mathbf{R}) = k_1 k_2 \frac{4\pi^2 \omega}{c} |f(\mathbf{k}_1, \mathbf{k}_2; \mathbf{R})|^2$$

in terms of one of the ejection angles obtained by ECS and PSECS are close to each other. Here PSECS gives for the integrated cross section $\sigma = 2.77$ kb, while ECS gives $\sigma = 2.61$ kb [30]. The difference between these two values is much bigger than estimated numerical error of our calculations. The one-fold differential cross section (DCS) $\frac{d\sigma}{dE_1} = \frac{1}{3} \left(\frac{d\sigma^{(\Sigma)}}{dE_1} + 2 \frac{d\sigma^{(\Pi)}}{dE_1} \right)$, and its Σ_u and Π_u contributions (i.e., $\frac{1}{3} \frac{d\sigma^{(\Sigma)}}{dE_1}$ and $\frac{2}{3} \frac{d\sigma^{(\Pi)}}{dE_1}$), shown on Fig. 3(b) also demonstrate such a discrepancy. Our Π_u curve actually coincides with the full DCS

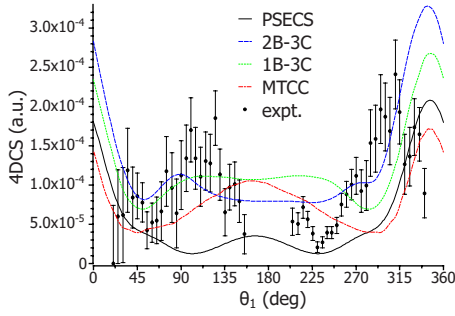


FIG. 4. (Color online) Nonaligned $H_2(e, 3-1e)$ 4DCS as a function of θ_1 for $E_i=612$ eV, $\theta_s=1.5^\circ$, $E_s=500$ eV, and $E_1=51$ eV. Our results (solid line), second (dashed line) and first (dotted line) Born 3C results [24], MTCC results [49](dash-dot line), and experimental data [48].

curve from [30]. On the other hand, the asymmetry parameter $\beta = \frac{2}{3} \left(\frac{d\sigma}{dE_1} \right)^{-1} \left(\frac{d\sigma^{(S)}}{dE_1} - \frac{d\sigma^{(M)}}{dE_1} \right)$, shown on the Fig. 3(b), calculated by PSECS differs from that of ECS by only 1%, which is within the numerical error. We cannot explain this noticeable difference in the DCS between our results and those of [30]. We must emphasize that convergence tests for each parameter of our numerical scheme (the number of angular basis functions, the size of radial grid step, the number of used terms in the Neumann's expansion, the radius of the space box, the complex scaling angle and turning point, and the amplitude extraction radius) show that the estimated numerical error of our results is in the limits of few percents, that is, much smaller than the observed difference with [30]. Anyhow, this difference is much less than the errors of existing experimental data [46,47].

To extend our procedure to the double ionization of H_2 by fast electron impact, we have calculated the fourfold differential cross section (4DCS)

$$\sigma^{(4)}(E_i, \theta_s, \phi_s, E_1, E_2, \theta_1, \phi_1) = \frac{d^4\sigma}{d\Omega_s dE_1 dE_2 d\Omega_1} = \oint \sigma^{(5)} d\Omega_2$$

of this process for randomly oriented H_2 molecules. We have chosen the same dynamical situation as in the unique $(e, 3-1e)$ experiment [48] to our knowledge. Here the incident electron energy $E_i=612$ eV, the scattered electron energy $E_s=500$ eV, the scattering angle $\theta_s=1.5^\circ$, only one of the two ejected electrons which has the energy $E_1=51$ eV is detected. The conservation of the energy permits us to deduce the energy of the unobserved ejected electron energy $E_2=10$ eV. We have determined the fivefold differential cross section (5DCS)

$$\begin{aligned} \sigma^{(5)}(E_i, \theta_s, \phi_s, E_1, \theta_1, \phi_1, E_2, \theta_2, \phi_2) \\ = \frac{d^5\sigma}{d\Omega_s dE_1 d\Omega_1 dE_2 d\Omega_2} = \frac{1}{4\pi} \oint \sigma^{(5)}(\mathbf{R}) d\Omega_R \end{aligned}$$

such that

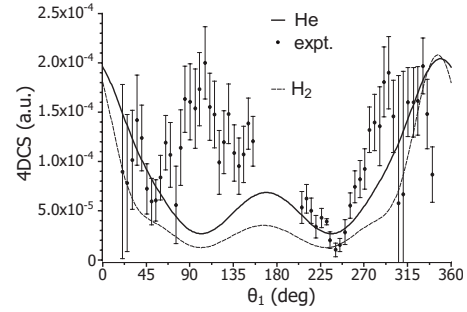


FIG. 5. $He(e, 3-1e)$ 4DCS as a function of θ_1 for $E_i=640$ eV, $\theta_s=1.5^\circ$, $E_s=500$ eV, $E_1=51$ eV. Our results (solid line), experimental data [48], and our H_2 results from Fig. 4(dashed line).

$$\sigma^{(5)}(E_i, \theta_s, \phi_s, E_1, \theta_1, \phi_1, E_2, \theta_2, \phi_2; \mathbf{R}) = \frac{k_1 k_2 k_s}{k_i} |f(\mathbf{k}_1, \mathbf{k}_2, \mathbf{K}; \mathbf{R})|^2$$

which gives the 5DCS for a fixed internuclear axis orientation. As we mentioned above only the two atomic electrons are treated by the *ab initio* procedure. Exchange between scattered and bound electrons is neglected and the action of this electron is taken into account through Eq. (9). The comparison of our results to the experimental data [48] and the earlier theoretical attempts [24,49], which are based on approximate functions for the ejected electrons, is shown in Fig. 4. The experimental data are given in arbitrary units. We have thus renormalized it to obtain best visual fit with our PSECS curve, which is given in atomic units. Curiously, the results of 3C shown on the curve [24] is close to our PSECS ones, not only in shape but in magnitude also. We chose between the numerous MTCC curves in [49] the one with $\varepsilon_i = -0.2/k_i$, which is the nearest to our curve in magnitude. It seems that, the disagreement of theory with experiment in position and relative magnitude of peaks is caused by the sequential mechanism of the double ionization, where the second Born interactions, which are not taken into account in our and all earlier attempts, could be important. During this process the incoming electron knocks out each target electron independently in contrast to the simultaneous double ionization where the incident electron ejects an electron and the shake off mechanism causes the ejection of the second.

The dependence of 4DCS on the nature of the target is of additional interest. In Fig. 5 we show our results for the $(e, 3-1e)$ of helium compared to the experimental results of

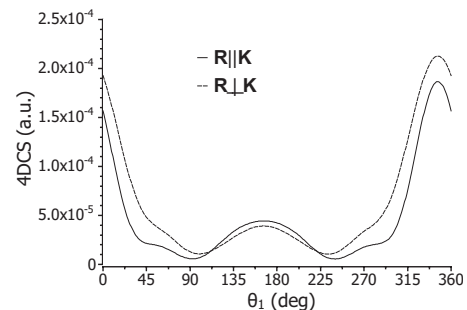


FIG. 6. The same as on Fig. 4 but for aligned molecule: $\mathbf{R} \parallel \mathbf{K}$ (solid line) and $\mathbf{R} \perp \mathbf{K}$ (dashed line).

[48] and our H_2 results from Fig. 4. It can be seen that, helium and H_2 curves are very close to each other. This confirms what is observed experimentally [48] that is the two-center character of H_2 is not manifested in 4DCS in such experiment conditions. This is not the consequence of averaging over the molecular axis direction \mathbf{n}_R as one might expect. From Fig. 6 it is clear that 4DCS is very weakly dependent on the internuclear axis direction.

IV. CONCLUSION

We have extended the recently developed *ab initio* method using the driven Schrodinger equation and external complex scaling method [28–30] to the simple and double ionization of H_2 by fast electron impact using prolate spheroidal coordinates which possess naturally the symmetry of the diatomic systems. Our procedure which combines the

advantages of ECS and the use of prolate spheroidal coordinates, confirms existing results on the simple ionization of He and H_2 , and double photoionization results on H_2 . Comparing our results with ($e, 3-1e$) experimental data demonstrates the significance of higher order processes for mean energy electron impact. In the future we will develop this method in a way to take into account the contribution of the sequential double ionization to ($e, 3-1e$) process.

ACKNOWLEDGMENTS

The authors are grateful to Prof. V. V. Derbov, Dr. O. Chuluunbaatar and Prof. V. V. Vinitzky for help and useful discussions. This work was supported by CRDF BRHE (Grant No. REC-006 SR-006-X1/B75M06 Y3-P-06-08), RFBR (Grant No. 08-01-00604a), and Celevaja Programma “Razvitie potenciala vysshej shkoly.”

-
- [1] T. Iijima, R. A. Bonham, and T. Ando, *J. Phys. Chem.* **67**, 1472 (1963).
 [2] C. Bottcher, *Chem. Phys. Lett.* **4**, 320 (1969).
 [3] E. S. Chang and U. Fano, *Phys. Rev. A* **6**, 173 (1972).
 [4] M. Shugard and A. U. Hazi, *Phys. Rev. A* **12**, 1895 (1975).
 [5] E. McCarthy, *J. Phys. B* **6**, 2358 (1973).
 [6] K. Jung, E. Schubert, D. A. L. Paul, and H. Ehrhard, *J. Phys. B* **8**, 1330 (1975).
 [7] E. Weigold, S. T. Hood, I. E. McCarthy, and P. J. O. Teubner, *Phys. Lett.* **44**, 531 (1973).
 [8] A. Crowe and J. W. McConkey, *J. Phys. B* **6**, 2088 (1973).
 [9] M. Cherid, A. Lahmam-Bennani, A. Duguet, R. W. Zuraes, R. R. Lucchese, M. C. Dal Cappello, and C. Dal Cappello, *J. Phys. B* **22**, 3483 (1989).
 [10] A. Duguet, A. Lahmam-Bennani, M. Lecas, and B. El Marji, *Rev. Sci. Instrum.* **69**, 3524 (1998).
 [11] M. Dürr, C. Dimopoulou, A. Dorn, B. Najjari, I. Bray, D. V. Fursa, Zhangjin Chen, D. H. Madison, K. Bartschat, and J. Ullrich, *J. Phys. B* **39**, 4097 (2006).
 [12] R. Dörner *et al.*, *Phys. Rev. Lett.* **81**, 5776 (1998).
 [13] Y. Muramatsu *et al.*, *Phys. Rev. Lett.* **88**, 133002 (2002).
 [14] M. Takahashi, J. P. Cave, and J. H. D. Eland, *Rev. Sci. Instrum.* **71**, 1337 (2000).
 [15] T. J. Reddish, G. G. Richmond, G. W. Bagley, J. P. Wightman, and S. Cvejanovic, *Rev. Sci. Instrum.* **68**, 2685 (1997).
 [16] T. Weber *et al.*, *Nature (London)* **431**, 437 (2004); *Phys. Rev. Lett.* **92**, 163001 (2004).
 [17] M. Gisselbrecht, M. Lavollée, A. Huetz, P. Bolognesi, L. Avaldi, D. P. Seccombe, and T. J. Reddish, *Phys. Rev. Lett.* **96**, 153002 (2006).
 [18] J. Hanssen, B. Joulakian, R. D. Rivarola, and R. J. Allan, *Phys. Scr.* **53**, 41 (1996).
 [19] P. Weck, B. Joulakian, and P. A. Hervieux, *Phys. Rev. A* **60**, 3013 (1999).
 [20] P. Pluvinage, *Phys. Radium* **12**, 789 (1951).
 [21] B. Joulakian, J. Hanssen, R. D. Rivarola, and A. Motassim, *Phys. Rev. A* **54**, 1473 (1996).
 [22] M. Walter and J. Briggs, *J. Phys. B* **32**, 2487 (1999).
 [23] P. F. Weck, O. A. Fojón, B. Joulakian, C. R. Stia, J. Hanssen, and R. D. Rivarola, *Phys. Rev. A* **66**, 012711 (2002).
 [24] A. Mansouri, C. Dal Cappello, S. Houamer, I. Charpentier, and A. Lahmam-Bennani, *J. Phys. B* **37**, 1203 (2004).
 [25] C. Dal Cappello, A. Mansouri, S. Houamer, and B. Joulakian, *J. Phys. B* **39**, 2431 (2006).
 [26] A. S. Kheifets, *Phys. Rev. A* **71**, 022704 (2005).
 [27] V. V. Serov, V. L. Derbov, B. B. Joulakian, and S. I. Vinitzky, *J. Phys. B* **38**, 2765 (2005).
 [28] W. Vanroose, F. Martin, T. N. Rescigno, and C. W. McCurdy, *Phys. Rev. A* **70**, 050703(R) (2004).
 [29] W. Vanroose, F. Martin, T. N. Rescigno, and C. W. McCurdy, *Science* **310**, 1787 (2005).
 [30] W. Vanroose, D. A. Horner, F. Martin, T. N. Rescigno, and C. W. McCurdy, *Phys. Rev. A* **74**, 052702 (2006).
 [31] C. W. McCurdy, M. Baertschy, and T. N. Rescigno, *J. Phys. B* **37**, R137 (2004).
 [32] B. Simon, *Phys. Lett. A* **71**, 211 (1979).
 [33] T. N. Rescigno, M. Baertschy, and C. W. McCurdy, *Phys. Rev. A* **68**, 020701(R) (2003).
 [34] M. Baertschy, T. N. Rescigno, and C. W. McCurdy, *Phys. Rev. A* **64**, 022709 (2001).
 [35] L. Tao, C. W. McCurdy, and T. N. Rescigno, *Phys. Rev. A* **79**, 012719 (2009); **80**, 013402 (2009).
 [36] J. Budziński and S. Prajsnar, *J. Chem. Phys.* **101**, 10783 (1994).
 [37] We used CLPMN and CLQMN subroutines for calculation of first- and second kind Legendre functions of complex argument. Acknowledge to copyright of <http://jin.ece.uiuc.edu/routines/routines.html>
 [38] P. M. Morse and H. Feshbach, *Methods of Theoretical Physics, Part II* (McGraw-Hill, New York, 1953), pp. 1502–1512.
 [39] I. V. Komarov, L. I. Ponomarev, and S. Yu. Slavyanov, *Spheroidal and Coulomb Spheroidal Functions* (Nauka, Moscow, 1976).
 [40] L. I. Ponomarev, I. V. Puzynin, and T. P. Puzynina, *J. Comput. Phys.* **13**, 1 (1973).
 [41] J. Sims and S. Hagstrom, *J. Chem. Phys.* **124**, 094101 (2006).

- [42] J. A. R. Samson and G. N. Haddad, *J. Opt. Soc. Am. B* **11**, 277 (1994).
- [43] V. V. Serov, V. L. Derbov, B. B. Joulakian, and S. I. Vinitzky, *Phys. Rev. A* **75**, 012715 (2007).
- [44] A. Kheifets, I. Bray, A. Lahmam-Bennani, A. Duguet, and I. Taouil, *J. Phys. B* **32**, 5047 (1999).
- [45] I. Sánchez and F. Martín, *J. Chem. Phys.* **110**, 6702 (1999).
- [46] G. Dujardin, M. J. Besnard, L. Hellner, and Y. Malinovitch, *Phys. Rev. A* **35**, 5012 (1987).
- [47] H. Kossmann, O. Schwarzkopf, B. Kämmerling, and V. Schmidt, *Phys. Rev. Lett.* **63**, 2040 (1989).
- [48] A. Lahmam-Bennani, A. Duguet, and S. Roussin, *J. Phys. B* **35**, L59 (2002).
- [49] O. Chuluunbaatar, B. B. Joulakian, I. V. Puzynin, Kh. Tsookhuu, and S. I. Vinitzky, *J. Phys. B* **41**, 015204 (2008).